

Evaporation Duct Effects on Sea Clutter

RICHARD A. PAULUS

Abstract—Existing sea clutter models are in general agreement on the trends and magnitudes of sea reflectivity at low (1° – 10°) grazing angles. However, at extremely low grazing angles ($< 1^\circ$), models, theory, and measurements show considerable differences. The effects of the oceanic evaporation duct on grazing angle are investigated. Significant changes in grazing angle due to the evaporation duct are found and the illumination of the sea surface by the radar is shown to extend well beyond the standard ($4/3$ earth) radar horizon range. A series of sea clutter model comparisons shows that much of the difference between models can be attributed to evaporation duct effects.

I. INTRODUCTION AND BACKGROUND

ONE PHENOMENON with which naval radars must contend is sea clutter return. This return is usually unwanted and masks the return from desired targets, particularly low-flying, small radar-cross-section targets. Sea clutter is generally accepted to be dependent upon radar wavelength, polarization, angle of incidence, sea state, and wind (wave) direction relative to the radar antenna [1]. Wind and sea conditions are either assumed to be highly correlated or can be specified separately. Theory, models, and measurements show reasonable agreement at low grazing angles ($\sim 1^\circ$ to 10°) but disagree markedly at lower grazing angles ($< 1^\circ$), particularly at low sea states.

Two sea clutter models, among several, appear to be suitable to the low grazing angles and frequency limits required in the surface search radar problem.

The Georgia Institute of Technology has developed a deterministic parametric model for the average radar cross section per unit area (reflectivity) of the sea [1]. The model is a function of grazing angle, wind speed and/or average wave height, angle between wind (sea) direction and antenna bore-sight, radar wavelength, and polarization. This model, hereafter referred to as the GIT model, is shown in Table I. The average clutter cross section per unit area is shown to be the product of a multipath factor A_i , wind speed factor A_w , and wind (sea) direction factor A_u . A_i is a theoretically derived factor for multipath interference for a Gaussian distribution of wave heights with standard deviation σ_h . A_u and A_w were derived empirically. A_u describes the variation due to aspect angle between the antenna and sea direction. Wind and sea direction are assumed to be highly correlated as are wind speed and wave height. However, for changing conditions, wind speed and wave height could be considered as separate data.

The Technology Service Corporation developed a model

Manuscript received November 22, 1988; revised April 9, 1990.
The author is with the Ocean and Atmospheric Sciences Division, Naval Ocean Systems Center, Code 543, San Diego, CA 92152-5000.
IEEE Log Number 9038570.

TABLE I
GIT SEA CLUTTER MODEL [1]

λ - radar wavelength (m)	ϕ - wind direction (deg)
ψ - grazing angle (rad)	V_w - wind speed (m/s)
h_{av} - average wave height (m)	
Interference factor:	
$\sigma_\phi = (14.4\lambda + 5.5) \psi h_{av} / \lambda$	
$A_i = \sigma_\phi^4 / (1 + \sigma_\phi^4)$	
Upwind/downwind factor:	
$A_u = \exp \{ 0.2 \cos \phi (1 - 2.8 \psi) (\lambda + 0.02)^{-0.4} \}$	
Wind speed factor:	
$q_w = 1.1 / (\lambda + 0.02)^{0.4}$	
$h_{av} = \left(\frac{V_w}{8.67} \right)^{2.5}$	
$A_w = [1.9425 V_w / (1 + V_w / 15)]^{q_w}$	
Reflectivity:	
$\sigma_{HH}^0 = 10 \log (3.9 \times 10^{-6} \lambda \psi^{0.4} A_i A_u A_w)$	
Polarization adjustment:	
(frequency ≥ 3000 MHz)	
$\sigma_{VV}^0 = \sigma_{HH}^0 - 1.05 \ln (h_{av} + 0.02) + 1.09 \ln (\lambda) + 1.27 \ln (\psi + 0.0001) + 9.70$	
(frequency < 3000 MHz)	
$\sigma_{VV}^0 = \sigma_{HH}^0 - 1.73 \ln (h_{av} + 0.02) + 3.76 \ln (\lambda) + 2.46 \ln (\psi + 0.0001) + 22.2$	

(W. Rivers, private communication, 1987) that is based on a fit to data compiled by Nathanson [2]. This model, hereafter referred to as the TSC model, is a function of grazing angle, Douglas sea state number, wind aspect angle, radar wavelength, and polarization. The TSC model is similar to the GIT model in functional form.

Both models show similar trends in reflectivity:

- 1) Reflectivity increases with sea state, frequency, and grazing angle.
- 2) Reflectivity upwind is approximately 5 dB greater than downwind; crosswind values are approximately midway between the upwind and downwind values.
- 3) Reflectivity for vertical polarization is generally greater than horizontal, particularly for low sea states. As sea state increases, reflectivity for horizontal polarization may exceed that for vertical polarization, particularly at low grazing angles ($< 1^\circ$).

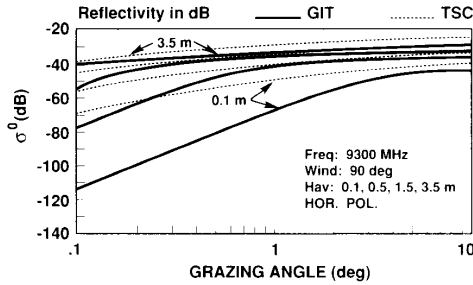


Fig. 1. Comparison of reflectivity for GIT and TSC models parametric in average wave height; frequency is 9300 MHz, horizontal polarization, and crosswind aspect.

For average wave heights of 0.5 m or greater and grazing angles greater than 1° , the GIT and TSC models are in substantial agreement. However, for lower wave heights and grazing angles, the TSC model yields values of reflectivity as much as 50 dB greater than the GIT model (Fig. 1). These differences have been attributed to heavy averaging done by Nathanson [1].

However, other factors may contribute to the disparities at extremely low grazing angles. The effects of the low-level refractive structure over the ocean is one possible factor. In a maritime environment, there are two types of surface duct phenomena that can significantly affect propagation in the radar bands: the surface-based duct and the evaporation duct [3].

A sea clutter model for surface-based ducts has been proposed [4] that, at least qualitatively, accounts for sea clutter effects under surface-based duct conditions. However, the annual occurrence of surface-based ducts over the ocean is only 8% [5].

The evaporation duct, which is formed by the interactions between the lower atmosphere and the ocean surface, is nearly always present over the ocean, due mainly to the strong moisture gradient in the first few meters above the surface. Since the vertical scale of the evaporation duct is on the order of a few tens of meters, its effects on microwave propagation are frequency dependent, with a practical lower limit of 1–2 GHz for radar range enhancements along the surface. Under certain infrequent oceanographic and meteorological conditions, the evaporation duct may vanish or a subrefractive condition may be present.

This paper will consider the GIT and TSC sea clutter models and the effect the evaporation duct could have on sea clutter returns.

II. STRUCTURE OF THE EVAPORATION DUCT

The evaporation duct is a result of the temperature and water vapor pressure profiles in the surface layer of the marine atmosphere. Due to air-sea interaction effects, the air temperature over the open ocean is generally slightly less than or just equal to the sea surface temperature. However, the water vapor pressure at the sea surface is at saturation because of continuity reasons and the ambient water vapor pressure a few meters above the surface is generally at a level of 70–90% of the surface value. The result is a gradient of

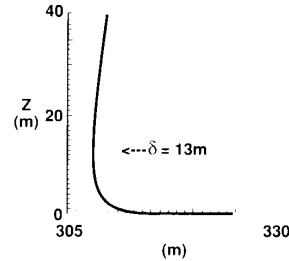


Fig. 2. Example of a modified refractivity M profile for a 13 m evaporation duct. M_0 is 325 and δ is duct height.

refractivity that may meet the criteria for trapping of electromagnetic waves. The evaporation duct varies in height and strength with meteorological and oceanographic conditions.

A model for the refractivity profile in the surface layer of the marine atmosphere that has been used for propagation modeling purposes is a logarithmic profile calculated from sea temperature, air temperature, relative humidity, and wind speed [6]. Expressing this profile in terms of modified refractivity as a function of evaporation duct height yields (see Appendix):

$$M(z) = M_0 + 0.125z - 0.125\delta \ln \left(\frac{z + z_0}{z_0} \right) \quad (1)$$

where M_0 is the value of M at the sea surface, z is the height in meters, and δ is evaporation duct height in meters. The aerodynamic roughness length z_0 is assumed to be a constant equal to 1.5×10^{-4} m. An example M profile is shown in Fig. 2. Logarithmic profiles begin to be less representative of real conditions in the atmosphere at heights greater than 20–30 m. Statistics on the evaporation duct have been compiled and are available in IBM PC compatible computer data base format [5].

III. EVAPORATION DUCTING EFFECTS ON SEA CLUTTER

The effects of low-level ducting on sea clutter have been qualitatively explained [7]. Surface-based ducts from evaluated refractive layers tend to produce enhanced clutter "rings" at discrete ranges well beyond the standard horizon. Evaporation ducts generally produce continuous enhanced clutter within and extending beyond the standard horizon. Experimental X-band radar data that appear to be consistent with what one expects of evaporation duct clutter is reproduced in Fig. 3 [8]. The ducting reflectivity data decrease with decreasing grazing angle at a lesser rate than the non-ducting data; the latter tend to agree with the GIT model predictions. Another significant feature of Fig. 3 is the manner in which the data are displayed. Sea clutter power is experimentally measured as a function of range by a radar at a known height above the sea surface. In order to transform these data to a function of grazing angle, the refractive structure must be known, or assumed. The usual procedure is to assume a standard atmosphere (4/3 earth). Thus, it is likely that much of the clutter data are "contaminated" by evaporation ducting effects that would represent something other than a standard atmosphere.

If one assumes that the GIT model represents standard

atmosphere conditions and the TSC model represents practical conditions, then a modification of the GIT model to account for evaporation ducting should bound the TSC model when applied to the range of typical evaporation duct heights.

The GIT model in fact allows for a duct height constant [1]. The grazing angle is first determined from

$$\psi' = h/1000R - R/2A_e \quad (2)$$

where h is radar antenna height in meters, R is range in kilometers, and A_e is effective earth radius in kilometers. This initial grazing angle is adjusted by frequency and duct height constant according to

$$\psi = (\psi'^2 + (\lambda/4d)^2)^{1/2} \quad (3)$$

where d is the duct height constant in meters. This adjustment may appear to work in some cases. However, if d is assumed to be a parameterization of the evaporation duct, (2) and (3) are physically unrealistic. The first difficulty is in determining an appropriate A_e for a ducting situation. The second difficulty is that one would expect ψ to approach ψ' as duct height goes to zero; the opposite happens in (3).

An alternative to a duct height constant is to consider how the presence of a refractive structure different from the standard atmosphere would affect grazing angle. It has been previously demonstrated that logarithmic and exponential refractive profiles in the surface layer extended illumination along the surface and reduce the rate of decrease of grazing angle with range [9].

Given an M profile (1), ray trace techniques can be used to determine grazing angle at the surface versus range. The maximum range at which a ray can strike the surface is the limiting range of the ray trace technique R_{lim} . The method for determining R_{lim} is to first determine the height at which the minimum M value occurs; this height is δ for $\delta \geq 0$. If the height of the radar antenna is greater than or equal to δ , the elevation angle at the radar for the limiting ray is

$$\alpha_h = -[(2 \times 10^{-6})(M_{ant} - M_{min})]^{1/2} - 1 \times 10^{-6} \text{ rad} \quad (4)$$

where M_{ant} is the value of M at the antenna height and M_{min} is the minimum value of M on the profile. If the height of the radar antenna is less than δ , then the elevation angle is the positive value of α_h . This is shown schematically in Fig. 4.

Using geometric optics, one obtains grazing angle ψ versus range as in Fig. 5. The effects of using a logarithmic refractivity profile instead of a standard atmosphere profile ($dM/dh = 0.118 \text{ M/m}$) are to change the variation of grazing angle with range and change the range to the "horizon." For a standard atmosphere ($\delta = 0 \text{ m}$) and a 25 m antenna height, grazing angle decreases to 0.1° by 10.6 km. For a commonly occurring evaporation duct of 10 m, the grazing angle approaches 0.3° at 10 km and decreases only slightly with range over the next 60 km. Using a grazing angle of 0.3° at 10 km instead of 0.1° yields, for a 0.1 m average

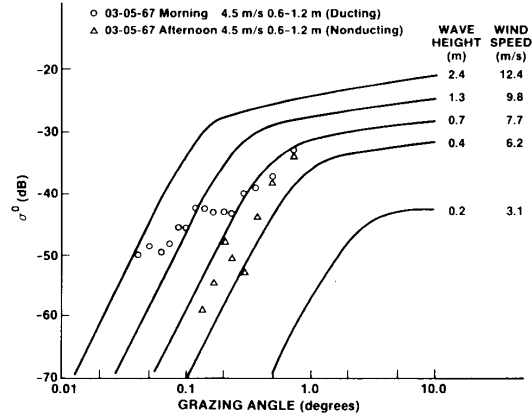


Fig. 3. Reflectivity measurements made under ducting and nonducting conditions compared to GIT model [8].

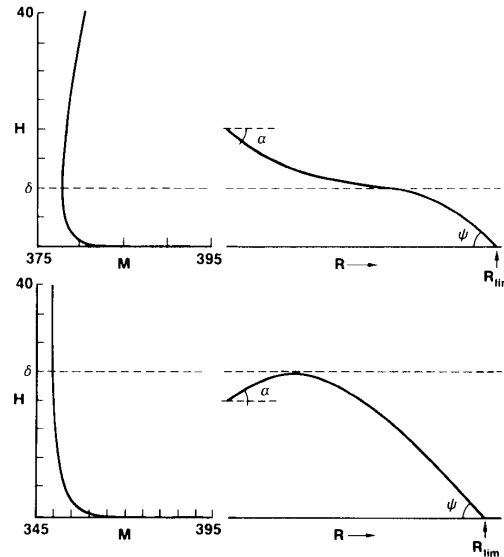


Fig. 4. Schematic of the determination of R_{lim} by ray trace techniques for radar antenna relative to the evaporation duct height. α is depression (or elevation) angle, ψ is grazing angle, and δ is evaporation duct height.

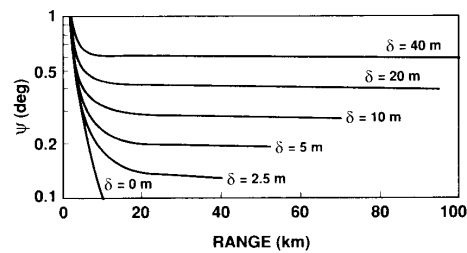


Fig. 5. Grazing angle, ψ , in degrees, versus range, parametric in evaporation duct height δ . Antenna height is 25 m.

wave height in Fig. 1, approximately a 20 dB increase in reflectivity over the standard atmosphere GIT model. This accounts for about half of the difference between the GIT and TSC models at low sea states; at higher sea states, a larger part of the difference is accounted for by nonstandard refrac-

tion. For a range of antenna heights typical of shipboard installations and a given evaporation duct height, there is only a slight variation of the grazing angle over that height range. This is because the refractive gradients at heights more than a few meters are small compared to the gradients in the lowest few meters (Fig. 2).

The range at which the curves in Fig. 5 stop is R_{lim} . The calculation of the limiting range can be quite sensitive to the implementation of ray tracing techniques. In addition, in those cases when the antenna is below the evaporation duct height, the limiting range may decrease with height. If the antenna is located above the evaporation duct height, then the limiting range increases monotonically with antenna height. Thus, the limiting range is more qualitative in showing horizon extension rather than quantitative in showing how far clutter is enhanced.

Fig. 6 compares, over frequency, the GIT and TSC models with the GIT model complemented with range and grazing angle calculations for the indicated evaporation duct heights. The GIT and TSC models stop at a standard atmosphere grazing angle of 0.1° . The evaporation ducts extend reflectivity well beyond the standard radar horizon of 20.6 km. The limiting range for the 30 m duct is off the scale at approximately 133 km. The trend of reflectivity levels in Fig. 6 is to increase with duct height, increasing faster at lower duct heights than at higher. Note that a 0 m evaporation duct would be virtually identical to the GIT model (standard atmosphere) and that a subrefractive profile would shorten the horizon and lower reflectivity values even further than the GIT model. Fig. 7 (along with Fig. 6(b)) compares, over wind speed (sea state), the three models. The evaporation duct effects do not bring reflectivity levels up to the TSC model at low wind speed but do at wind speeds of about 5 m/s and greater.

Fig. 1 compared the GIT and TSC models as a function of grazing angle; to include evaporation duct effects in a display like this requires using depression angle (i.e., angle below the horizontal at the radar antenna) to compare the models because grazing angle is a variable function of range in the evaporation duct model. Fig. 8 shows the variation of reflectivity with depression angle of the three models for two sea conditions and several evaporation duct heights. The 0 m evaporation duct represents the GIT standard atmosphere model. The evaporation duct effects appear at depression angles less than approximately one degree and the effects are larger for low seas than for higher seas. Reflectivity for a given evaporation duct and sea condition varies only slightly at small depression angles ($< 0.15^\circ$).

The evaporation duct heights used in Figs. 6, 7, and 8 were chosen based on a range of duct heights climatologically representative of world-wide conditions [5]. These duct heights were derived from data reported by transiting ships.

Equation (1) assumes thermally neutral conditions. Although "near-neutral" conditions are a good assumption in the open ocean, conditions in coastal and offshore areas may vary considerably away from neutral. There is an infinite combination of sea temperature, air temperature, relative humidity, and wind speed that will yield a given duct height.

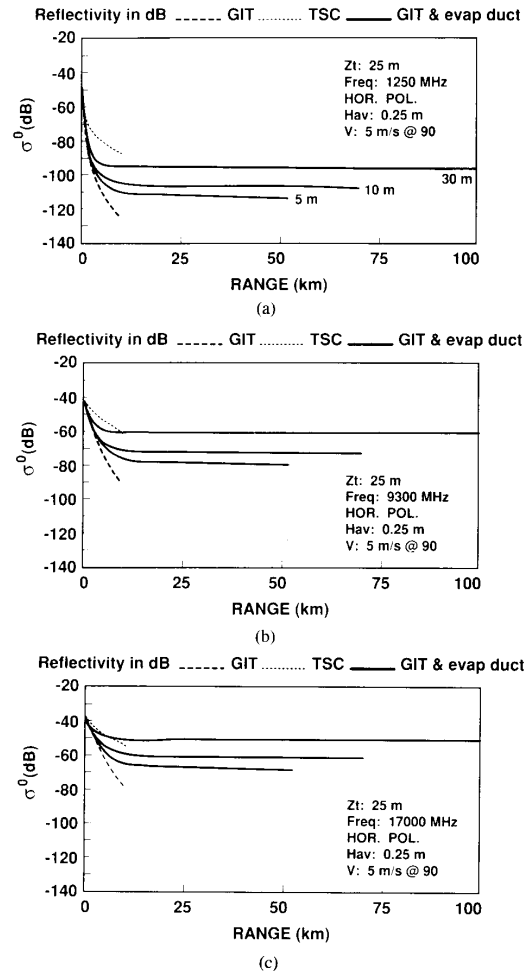


Fig. 6. (a) Comparison of models of reflectivity versus range for GIT, TSC, and GIT modified by ray trace calculations for duct heights of 5, 10, and 30 m. Radar height is 25 m, horizontal polarization, 5 m/s wind, crosswind aspect, and frequency of 1250 MHz. (b) Same as (a), except frequency is 9300 MHz. (c) Same as (a), except frequency is 17 000 MHz.

The various combinations of these parameters results in a slight variation in the shape of the logarithmic profile for a given duct height that is a function of the stability of the surface layer. This variation would affect the grazing angles and ranges determined from geometric optics. There are not sufficient data available to estimate how much variation in grazing angle would result from stability effects for a particular geographic area.

There are also other difficulties with the grazing angle modification approach. First, ray trace techniques are independent of frequency. The effects of the evaporation duct on propagation are highly frequency dependent, with high frequencies (X-band and above) more easily enhanced than lower frequencies (S-band and below). The lower limit of effectiveness of evaporation ducting (based on the occurrence of sufficiently strong ducts) is $\sim 1-2$ GHz. It is reasonable to expect a similar behavior in the backscatter propagation;

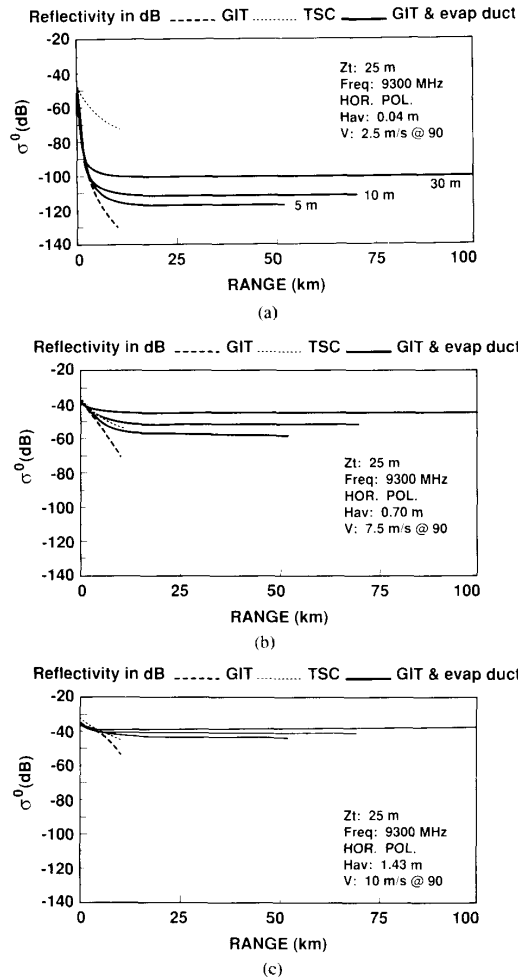


Fig. 7. Comparison of models of reflectivity versus range for GIT, TSC, and GIT modified by ray trace calculations for duct heights of 5, 10, and 30 m. Radar height is 25 m, horizontal polarization, frequency of 9300 MHz, crosswind aspect, and 2.5 m/s wind speed. (b) Same as (a), except 7.5 m/s wind speed. (c) Same as (a), except 10 m/s wind speed.

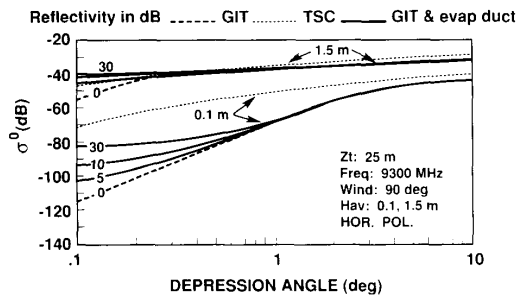


Fig. 8. Comparison of models of reflectivity versus depression angle for GIT, TSC, and GIT modified by ray trace calculations for a 25 m antenna, evaporation duct heights of 0, 5, 10, and 30 m, and two wave conditions.

thus, one would not expect clutter at S-band to be extended as far as the clutter for X-band for a given duct. Yet, R_{lim} for a given duct height, is the same for all frequencies.

Another difficulty lies at the limiting range of the ray trace. What is the behavior of σ^0 beyond R_{lim} ? This is the region beyond the validity of geometric optics where only physical optics is valid. The grazing angle at R_{lim} for a given duct is in quite close agreement with the real part of the eigenangle, referenced to the surface, of the dominant mode determined by waveguide calculations. This eigenangle varies only slightly with frequency over the range of interest (1–20 GHz). The physical optics analysis of reflectivity at ranges greater than R_{lim} is incomplete at this time.

To complete the determination of clutter within the ray-optics horizon, the normalized radar cross section, σ^0 is

multiplied by the area illuminated by the radar:

$$A_c = \frac{\theta_a R c \tau}{4 \ln 2} \sec \psi \quad \text{m}^2. \quad (8)$$

θ_a is horizontal beamwidth in radians, R is range in meters, c is the speed of light in m/s, τ is pulsewidth in seconds, and ψ is grazing angle in radians (for grazing angles $< 10^\circ$, $\sec \psi \approx 1$).

IV. SUMMARY

Two radar sea clutter models were compared and the discrepancies between the two at very low grazing angles ($< 1^\circ$) were examined. In one model (GIT), data that were obviously due to ducting effects were culled during its development; in the other model (Nathanson/TSC), most available data were utilized. The two models were found to differ markedly at low grazing angles. This difference had previously been attributed to averaging [1]. However, much of the difference between the models can be explained by postulating evaporation ducting effects in place of standard atmosphere propagation. Evaporation ducting effects on sea clutter quantitatively explain much of the difference between the GIT and TSC clutter models within the standard horizon due to the slower rate of decrease of grazing angle with range as compared to the standard (4/3 earth) refraction. Qualitatively, the presence of a logarithmic refractive profile extends the optical horizon beyond the standard radar horizon. It was shown in model comparisons that the GIT model, with a rather simple ray optics determination of grazing angle and range, could produce results commensurate with the TSC model.

Ray optics and the evaporation duct refractive structure do not provide a full solution to the sea clutter problem. The geometric optics approach is not frequency dependent; all radar bands are predicted to have clutter enhancement to the same range, contrary to the known frequency dependence of the evaporation ducting mechanism. This seems intuitively incorrect, but no data are available to support or refute the frequency dependence of clutter range extension. Another unresolved problem is the behavior of clutter beyond the region of validity of ray theory.

The implication of the oceanic evaporation duct on experimental sea clutter measurements is that clutter data cannot be normalized assuming a 4/3 earth radius grazing angle. This is a complicating factor. On the positive side, radar detection models can be enhanced by utilizing evaporation duct height distributions [5] in combination with geometric optics to more realistically model sea clutter levels and the variation with ducting conditions.

APPENDIX

Refractive index n of the atmosphere is often expressed in terms of refractivity, $N = (n - 1) \times 10^6$, or modified refractivity, $M = N + 0.157z$, where z is height in meters [3]. Refractivity can be measured directly with a refractometer or derived from measurements of pressure, P (mb), temperature, T ($^\circ\text{K}$), and water vapor pressure, e (mb),

using

$$N = \frac{77.6P}{T} + 3.73 \times 10^5 \frac{e}{T^2}. \quad (9)$$

In the atmospheric surface layer, potential refractivity

$$\phi = \frac{77.6P_0}{\theta} + 3.73 \times 10^5 \frac{e_p}{\theta^2} \quad (10)$$

is a convenient parameter because of its conservative property in a dynamic atmosphere. Here θ is potential temperature and e_p is potential water vapor pressure, and P_0 is a reference pressure level (taken to be 1000 mb) [6].

There are several formulations for profiles of conservative properties in the atmospheric surface layer; for simplicity, the following formulation [10] is used:

$$\phi - \phi_0 = \frac{\phi^*}{\kappa} \left[\ln \left(\frac{z + z_0}{z_0} \right) - \psi_\phi \left(\frac{z + z_0}{L} \right) \right] \quad (11)$$

where ϕ_0 is the value of potential refractivity ϕ at the sea surface, based on the sea surface temperature and the saturation water vapor pressure at that temperature; ϕ^* is a scaling parameter assumed to be a constant for a given set of conditions; κ is von Karman's constant; z is height; z_0 is the aerodynamic roughness length; ψ_ϕ is a stability function, which, for neutral conditions (air temperature \approx sea temperature), is zero. The vertical derivative of (11) yields the gradient of ϕ

$$\frac{d\phi}{dz} = \frac{\phi^*}{\kappa(z + z_0)}. \quad (12)$$

From geometric optics, the critical gradient required for trapping is that which yields a ray curvature equal to the earth's curvature

$$\frac{dN}{dz} = -\frac{10^6}{a} = -0.157 \text{ N/m} \quad (13)$$

where a is earth radius in meters. Taking the total derivatives of $N(P, T, e)$ and $\phi(\theta, e_p)$ with respect to z and assuming that $\theta \approx T$ and $e_p \approx e$ in the surface layer yields

$$\frac{d\phi}{dz} = \frac{dN}{dz} - \frac{\partial N}{\partial P} \frac{dP}{dz}. \quad (14)$$

The partial derivative $\partial N / \partial P = 77.6/T$ varies from 0.28 to 0.26 mb^{-1} over the range of temperature 0° to 30°C . The derivative dP/dz can be evaluated by making the hydrostatic approximation

$$\frac{dP}{dz} = -\rho g = -\frac{Pg}{RT} \quad (15)$$

where ρ is density, g is acceleration of gravity (9.8 m/s^2), P is pressure (1000 mb), R is the individual gas constant for dry air ($2.87 \times 10^6 \text{ erg/g/}^\circ\text{K}$), and T is temperature. This yields a variation of dP/dz from -0.12 to -0.11 mb/m over the temperature range of 0° to 30°C . Taking the standard temperature (15°C), the critical gradient for trap-

ping, in terms of ϕ , is -0.125 m^{-1} and (12) becomes

$$-0.125 = \frac{\phi^*}{\kappa(\delta + z_0)} \quad (16)$$

where δ is the height at which this gradient occurs (evaporation duct height). Substituting for ϕ^* and taking $\phi = N + 0.032z = M - 0.125z$ in (11) gives an equation for the modified refractivity profile in terms of evaporation duct height and z :

$$M(z) = M_0 + 0.125z - 0.125(\delta + z_0) \ln \left(\frac{z + z_0}{z_0} \right) \quad (17)$$

where M_0 is the value of M at the sea surface, z is height in meters and δ is evaporation duct height in meters. The aerodynamic roughness length z_0 is taken to be 1.5×10^{-4} m. The roughness length is often neglected when added to δ .

REFERENCES

- [1] M. M. Horst, F. B. Dyer, and M. T. Tuley, "Radar sea clutter model," in *Proc. IEEE Int. Conf. Antennas Propagat.*, London, Nov. 1978, pp. 6-10.
- [2] F. E. Nathanson, *Radar Design Principles*. New York: McGraw-Hill, 1969.
- [3] H. V. Hitney, J. H. Richter, R. A. Pappert, K. D. Anderson, and G. B. Baumgartner, Jr., "Tropospheric radio propagation assessment," *Proc. IEEE*, vol. 73, no. 2, pp. 265-283, Feb. 1985.
- [4] F. P. Snyder, "A radar sea clutter model for atmospheric ducting conditions," Naval Ocean Syst. Cen., San Diego, CA, Tech. Doc. 721, Aug. 1984.
- [5] H. V. Hitney, A. E. Barrios, and G. E. Lindem, "Engineer's refractive effects prediction system (EREPS), revision 1.00 user's manual," Naval Ocean Syst. Cen., San Diego, CA Tech. Doc. 1342, July 1988.
- [6] H. V. Hitney, "Propagation modeling in the evaporation duct," Naval Electronics Lab. Cen. (now Naval Ocean Syst. Cen.), San Diego, CA, Tech. Rep. 1947, Apr. 1, 1975.
- [7] F. P. Snyder, "Radar clutter under atmospheric ducting conditions," in *Proc. Conf. Atmosph. Refractive Effects Assessment*, (Jan. 23-25, 1979) Naval Ocean Syst. Cen., San Diego, CA, Tech. Doc. 260, pp. 61-67.
- [8] F. B. Dyer and N. C. Currie, "Some comments on the characterization of radar sea clutter," in *Dig. Int. IEEE Symp. Antennas Propagat.*, June 10-12, 1974, pp. 323-326.
- [9] L. B. Wetzell, "A model for sea backscatter intermittency at extreme grazing angles," *Radio Sci.*, vol. 12, no. 5, pp. 749-756, Sept.-Oct. 1977.
- [10] H. A. Panofsky and J. A. Dutton, *Atmospheric Turbulence*. New York: Wiley, 1984.



Richard A. Paulus received the B.S. degree in meteorology from Iowa State University, Ames, in 1970, and the M.S. degree in meteorology and oceanography, with distinction, from the Naval Postgraduate School, Monterey, CA, in 1978.

Since 1982, he has been a member of the Ocean and Atmospheric Sciences Division of the Naval Ocean Systems Center, San Diego, CA, involved in radio climatology, atmospheric measurements, and modeling the effects of propagation through the troposphere on naval surveillance and communications systems.

Mr. Paulus is a member of the American Meteorological Society and Sigma Xi.